

A Mathematical Modal for Bingham Flow Properties of Blood in Narrow Tapered Tube

Arun Kumar Pandey and V. K. Chaubey

Department of Applied Science and Humanities
Buddha Institute of Technology, GIDA, Gorakhpur- 273209, India

E-mail: pandeyarun151281@gmail.com, vkcoct@gmail.com

Abstract: The stenosis and non-Newtonian property of the fluid in the blood flow represent the behavior of Herschel- Buckley fluid. In a tapered tube model all the vessels which carry blood towards the tissues are considered as long, slowly tapering cones rather than cylinders. Since the blood flow consist of two regions in which one is central region, consist of concentrated blood cells and its behavior is non-Newtonian and other region is peripheral layer of plasma which represent the Newtonian behavior of fluid motion. In present paper, we have considered the flow of blood through a uniform tapered tube which obeys the Bingham fluid model and obtained the condition for the wall shear stress and pressure gradient. Further in various graphs we represent the variation of shear stress at the wall and pressure gradient with respect to suspension concentration and tapered angle over the flow rate range 0.01 to 0.1 cc/sec.

Key Words: Newtonian fluid, blood flow, wall shear stress, tapered vessel, stenosis, Bingham model.

AMS(2010): 76D03, 76A05.

§1. Introduction

Womersley [14] introduced the concept of a tapered tube model for blood vessel and considered that all the vessels which carry blood towards the tissues should be long, slowly tapering cones rather than cylinders. Further Charm and Kurland [4] have examined the nature of blood flow in non-uniform capillary tubes which are relatively large diameter where the influence of a marginal gap is negligible, experimental values agree well with the anticipated value. But in cylindrical tubes where the influence of a marginal gap becomes important, the calculated and anticipated values diverge unless the probable gap width based on formulas validated in straight tubes. This conditions strongly suggests that marginal layers develop in tapered tubes similar to those in straight tubes.

Oka [9] has calculated the pressure development in a non-Newtonian flow through a tapered tube and obtained the distribution of pressure through tapered tube for Power law, Bingham

¹Received July 1, 2023, Accepted December 14, 2023.

body and Casson fluids. Chaturani and Pralhad [5] and Kumar and Kumar [5] have studied a steady laminar flow of blood in a uniform tapered tube by assuming blood as a polar fluid and obtained the analytical expressions for wall shear stress, pressure drop, total angular and axial velocities. Bagchi [1], Bugliarello and Sevilla [2], Chan [3], Chaturani and Palanisamy [6], Jianncing [7], Pappu and Bagchi [10], Pries and Secomb [11], Sakamoto et al. [12] and Singh and Kumar [13] have discussed the role of plasma peripheral layer on blood flow in capillaries.

In the present paper we have considered an anomalous behavior of blood flow through uniform tapered tubes and to understanding the complex rheological characteristics of blood flow we also considered Bingham blood model and obtained the expressions for the wall shear stress and pressure gradient. Further in various graphs we represent the variation of shear stress at the wall and pressure gradient with respect to suspension concentration and tapered angle over the flow rate range 0.01 to 0.1 cc/sec.

§2. The Mathematical Model

We considered a steady laminar flow of incompressible viscous non-Newtonian fluid model in a uniformly tapered tube of circular cross-section and the problem investigated under following assumptions:

- (i) Taper angle is very small;
- (ii) The motion is steady axisymmetric and in the z -direction;
- (iii) No body forces act in the fluid;
- (iv) The motion is so slow that inertia term can be neglected;
- (v) Pressure gradient is a function of axial co-ordinates only.

Further a section of tapered vessel is shown in Figure 1.

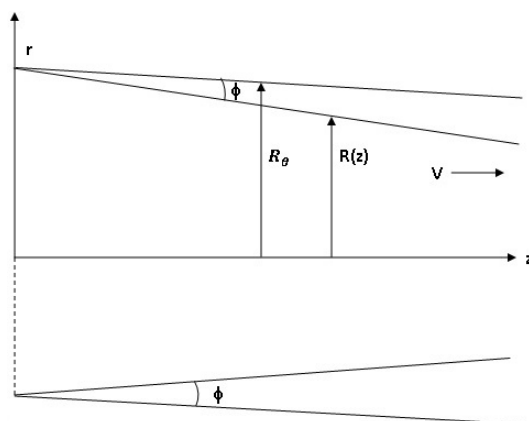


Figure 1. Geometry of the vessel

The radius of the tapered tube $R(z)$ is given by

$$R(z) = R_0 - z \tan \phi$$

where R_0 is the tube radius at $z = 0$, ϕ is the tapered angle and z the axis of the tapered tube.

2.1. Governing Equations. The governing equations in cylindrical co-ordinate system (r, z, θ) , which mathematically describe the laminar flow problem of an incompressible fluid are given by the continuity equation

$$\frac{\partial V_z}{\partial z} + \frac{\partial V_r}{\partial r} + \frac{V_r}{r} + \frac{1}{r} \frac{\partial V_\theta}{\partial \theta} = 0 \quad (2.1)$$

and the momentum equations

$$\begin{aligned} \rho \frac{DV_z}{Dt} = & -\frac{\partial p}{\partial z} + \frac{\partial}{\partial z} (2\mu \frac{\partial V_z}{\partial z}) + \frac{1}{r} \frac{\partial}{\partial \theta} [\mu (\frac{1}{r} \frac{\partial V_z}{\partial \theta} + \frac{\partial V_\theta}{\partial z})] + \\ & \frac{\partial}{\partial r} [\mu (\frac{\partial V_r}{\partial z} + \frac{\partial V_z}{\partial r})] + \frac{\mu}{r} (\frac{\partial V_r}{\partial z} + \frac{\partial V_z}{\partial r}), \end{aligned} \quad (2.2)$$

where $\frac{D}{Dt} = \frac{\partial}{\partial t} + V_r \frac{\partial}{\partial r} + V_z \frac{\partial}{\partial z} + \frac{V_\theta}{r} \frac{\partial}{\partial \theta}$.

Making use of the assumptions (ii), we have

$$\frac{\partial}{\partial t} = 0, \quad \frac{\partial}{\partial \theta} = 0, \quad V_r = V_\theta = 0, \quad V_z = V(r). \quad (2.3)$$

Using equation (2.3) in equation (2.2), we find the equations of motion and continuity for fully developed steady viscous incompressible laminar flow under no-body forces as

$$0 = -\frac{\partial p}{\partial z} + \frac{1}{r} \frac{\partial}{\partial r} (r\tau_{rz}), \quad (2.4)$$

$$0 = \frac{\partial p}{\partial r}, \quad (2.5)$$

$$\frac{\partial V}{\partial z} = 0, \quad (2.6)$$

where p is the pressure, V is the axial velocity and $\tau_{rz} = (\mu \frac{\partial V}{\partial r})$ the shear stress normal to r in z -direction.

2.2. Constitutive Equation. The constitutive equation for the shear stress τ and strain rate $\dot{\gamma}$ is given by

$$\tau = \tau_0 + \mu\dot{\gamma}; \quad \tau \geq \tau_0, \quad \text{and} \quad \dot{\gamma} = 0; \quad \tau \leq \tau_0, \quad (2.7)$$

where τ_0 is the yield stress, μ the coefficient of viscosity and $\dot{\gamma}$ the shear strain rate.

2.3. Boundary Conditions. The appropriate boundary conditions are given by

$$V = 0 \quad \text{at} \quad r = R(z), \quad (2.8)$$

$$\tau_{rz} = \tau_w \quad \text{at} \quad r = R(z), \quad (2.9)$$

$$V = V_p \quad \text{at} \quad r = R_p, \quad (2.10)$$

$$\tau_{rz} \text{ is finite at } r = 0, \quad (2.11)$$

where R_p is the plug radius and V_p the plug velocity.

2.4. Solution for Velocities, Volume Flow Rate and Wall Shear Stress.

(1) **Velocities.** Integrating equation (2.4) with the boundary condition (2.11), we get

$$\tau_{rz} = \frac{r}{2} \frac{\partial p}{\partial z}. \quad (2.12)$$

Making use of the equation (7) in equation (12), we have velocity equations as

$$\frac{dV}{dr} = \frac{1}{\mu} \left(\frac{\partial p}{\partial z} \frac{r}{2} - \tau_0 \right); \quad R_p \leq r \leq R(z), \quad (2.13)$$

$$\frac{dV_p}{dr} = 0; \quad 0 \leq r \leq R_p. \quad (2.14)$$

The plug flow exists whenever the shear stress does not exceed yield stress. Solving equations (2.13) and (2.14) with boundary conditions (2.8) to (2.10), we get

$$V = \frac{\tau_w(z)}{2\mu} R(z) \left[1 - \frac{r^2}{R^2(z)} - 2\beta \left(1 - \frac{r}{R(z)} \right) \right], \quad (2.15)$$

$$V_p = \frac{\tau_w(z)}{2\mu} R(z) (1 - \beta)^2, \quad (2.16)$$

where $\beta = \frac{\tau_0}{\tau_w(z)}$.

(2) **Volume Flow Rate and Wall Shear Stress.** The volume flow rate Q is given by

$$Q = Q_1 + Q_2, \quad (2.17)$$

where Q_1 and Q_2 are given by

$$Q_1 = \int_0^{R_p} 2\pi V_p r dr = \pi V_p R_p^2, \quad (2.18)$$

$$Q_2 = \int_{R_p}^{R(z)} 2\pi V r dr. \quad (2.19)$$

Now substituting the values of V_p and V from equations (2.15) and (2.16) in equations (2.18) and (2.19), we obtain

$$Q_1 = \frac{\pi}{2} \frac{\tau_w(z)}{\mu} R^3(z) (1 - \beta)^2, \quad (2.20)$$

$$Q_2 = \frac{\pi}{2\mu} \tau_w(z) R^3(z) \left[\frac{1}{2} - \frac{2}{3}\beta - \beta^2 + 2\beta^3 - \frac{5}{6}\beta^4 \right]. \quad (2.21)$$

Using equations (2.20) and (2.21) in equation (2.17), we have

$$Q = \frac{\pi}{4\mu} \tau_w(z) R^3(z) \left(1 - \frac{4}{3}\beta \right) \quad (2.22)$$

in where higher order of β are neglected.

Now from equation (2.12) and (2.22) with boundary condition (2.9), the pressure gradient

is obtained as

$$\frac{\partial p}{\partial z} = \frac{8\mu Q}{\pi R^4(z)} \left(1 + \frac{4}{3}\beta\right). \tag{2.23}$$

From equation (2.22) we have the shear stress at the wall as

$$\tau_w(z) = \frac{4\mu Q}{\pi R^3(z)} \left(1 + \frac{4}{3}\beta\right). \tag{2.24}$$

Now using equations (2.23) and (2.24), we have

$$\tau_w(z) = \frac{R(z)}{2} \frac{\partial p}{\partial z}. \tag{2.25}$$

Therefore, by the equations (2.23) and (2.24) we obtain that the pressure and the shear stress at the wall increases when $R(z)$ decreases.

§3. Results and Discussion

The pressure gradient and shear stress at the wall are given by the equation (2.23) and (2.25) respectively in which we observe that $\tau_w z$ and $\partial p/\partial z$ changes with z (along the tube axis), i.e. pressure gradient and wall shear stress increases with decrease in the radius of the tapered tube. Therefore we should not take the pressure gradient to be constant. Some authors have proposed a micro polar fluid model for blood flow through a small tapered tube and have assumed pressure gradient to be constant throughout the investigation, which is not true.

We consider the radius of tapered vessel $R_\theta = 100\mu m$. The variation of pressure gradient and shear stress at the wall are calculated, with the help of equations (2.23) and (2.24) for the flow rate over the range 0.02 to 0.10 cc/sec, for different tapered angles ($1^\circ \leq \theta \leq 2^\circ$) and the suspension concentrations 20%, 30% and 40% .

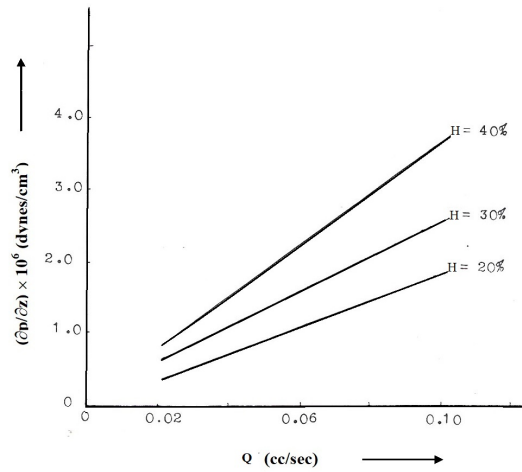


Figure 2. Variation of pressure gradient with flow rate for different suspension concentrations ($Z = 0.10cm, \phi = 1.4^\circ, R_\theta = 0.01cm$)

Figures 2, 3 and 4 show the variation of pressure gradient with flow rate for different suspension concentration, different tapered angle and different axial distance. From these Figures it is clear that pressure gradient increases with increase in axial distance, tapered angle and suspension concentration.

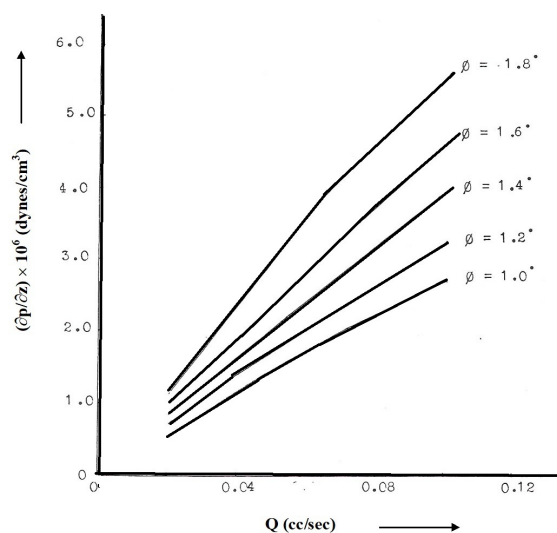


Figure 3. Variation of pressure gradient with flow rate for different tapered angles
($H = 4\%$, $R_\theta = 0.01\text{cm}$, $z = 0.10\text{cm}$)

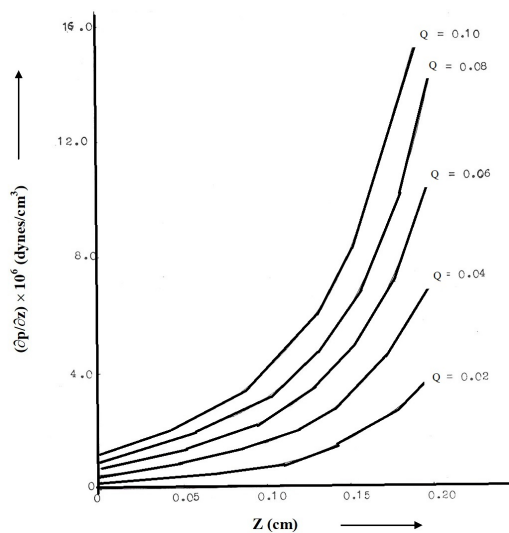


Figure 4. Variation of pressure gradient with axial distance for different flow rates
($R_\theta = 0.01\text{cm}$, $H = 40\%$, $\phi = 1.4^0$)

Now, Figures 5, 6 and 7 show the variation of shear stress at the wall with flow rate Q for different angles, axial distances and concentrations.

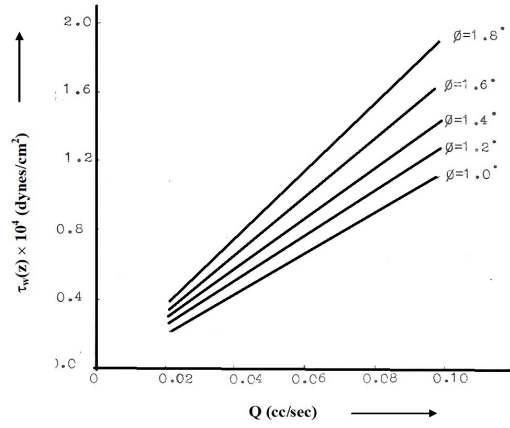


Figure 5. Variation of wall shear stress with flow rate for different tapered angles ($H = 40\%$, $R_\theta = 0.01\text{cm}$, $z = 0.10\text{cm}$)

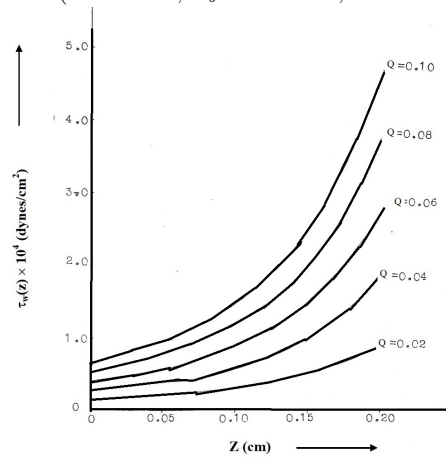


Figure 6. Variation of wall shear stress with axial distance for different flow rates ($H = 40\%$, $\phi = 1.4^0$, $R_\theta = 0.01\text{cm}$)

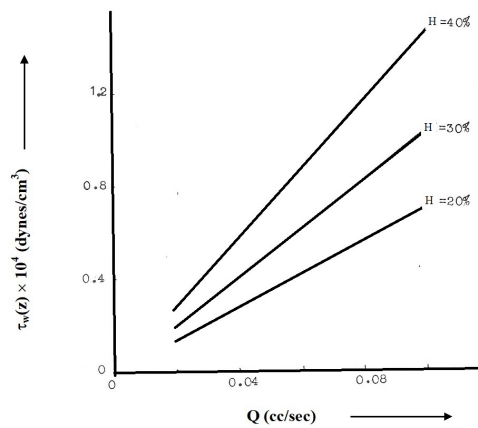


Figure 7. Variation of wall shear stress with flow rate for different hematocrit ($\phi = 1.4^0$, $z = 0.1\text{cm}$, $R_\theta = 0.01\text{cm}$)

From the above figures, it is clear that shear stress at wall increases with suspension concentration and tapered angles. $\tau_w z$ is an increasing function of axial distance. Thus, for known flow rate, the shear stress can be calculated at any point of the tapered tube. These fluid dynamics results could be very useful in understanding the vascular fluid mechanics. Now from Figures 8, 9 and 10 we have, for Newtonian fluid $\beta = 0$, the variation of pressure gradient with flow rate Q for different suspension concentrations, tapered angles and axial distances. We observe that the values of pressure gradient are less than those for Bingham fluid model. From these Figures, the same trends for pressure gradient are obtained as for Bingham fluids.

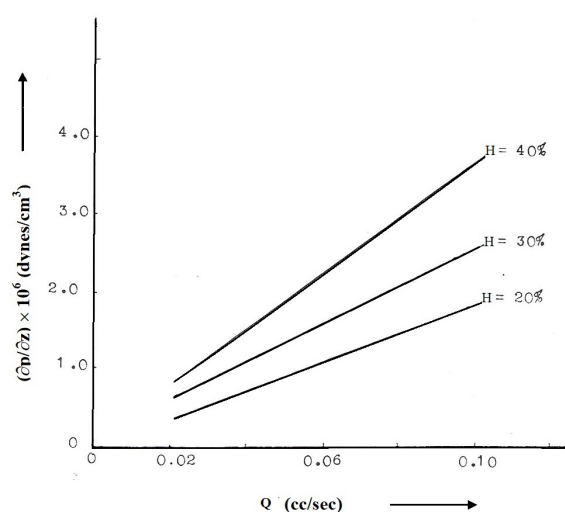


Figure 8. Variation of pressure gradient with flow rate different suspension concentration (Newtonian fluid with $\phi = 1.4^\circ$, $z = 0.10\text{cm}$, $R_\theta = 0.01\text{cm}$, $\beta = 0.0$)

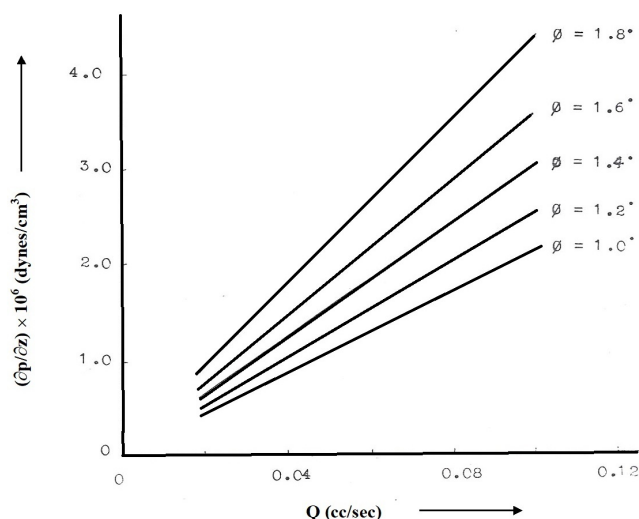


Figure 9. Variation of pressure gradient with flow rate for different tapered angles (Newtonian fluid with $H = 40\%$, $R_\theta = 0.01\text{cm}$, $z = 0.10\text{cm}$, $\beta = 0.0$)

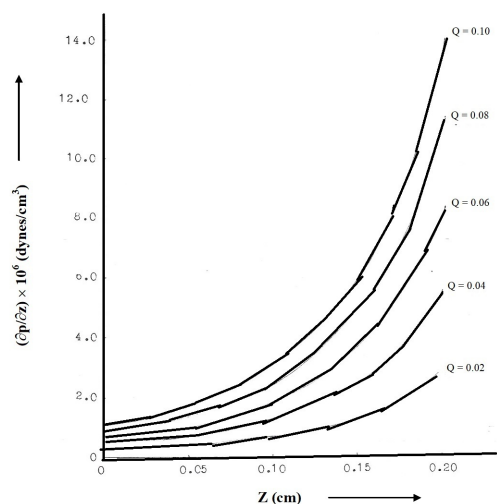


Figure 10. Variation of pressure gradient with axial distance for different flow rates (Newtonian fluid with $H = 40\%$, $R_\theta = 0.01\text{cm}$, $\phi = 1.4^\circ$, $\beta = 0.0$)

References

- [1] Bagchi P., Mesoscale simulation of blood flow in small vessels, *J. Biophysics* 92(6) (2007), 1858 C 1877, doi: 10.1529/biophysj.106.095042.
- [2] Bugliarello G. and Sevilla J., Velocity distribution and other characteristics of steady and pulsatile blood flow in fine glass tubes, *Biorheology*, 7(2)(1970), 85 C 107, doi: 10.3233/BIR-1970-7202.
- [3] Chan W. Y., *Simulation of Arterial Stenosis Incorporating Fluid Structural Interaction and Non-Newtonian Blood Flow*, Masters Thesis, RMIT University, Australia, 2006.
- [4] Charm S. E. and Kurland G. S., Blood flow in non-uniform tapered capillaries tubes, *Biorheology*, 4(4)(1967), 175-183, doi:10.3233/bir-1967-4404.
- [5] Chaturani P. and Pralhad R. N., Blood flow in tapered tube with bio-rheological applications, *Biorheology*, 22(4)(1985), 303-314.
- [6] Chaturani P. and Palanisamy V., Casson fluid model for pulsatile flow of blood with periodic body acceleration, *Biorheology*, 27(5)(1990), 619 C 630, doi:3233/bir1990-27501.
- [7] Jiannong Fang and Owens R. G., Numerical simulation of pulsatile blood flow using a new constitutive model, *Biorheology*, 43(5)(2006), 637 C 660.
- [8] Sanjeev Kumar and Sanjeet Kumar, A mathematical model for Newtonian and non-Newtonian flow through tapered tubes, *Indian Journal of Biomechanics*, Special Issue (NCBM 7-8) (2009), 191-195.
- [9] Oka S., Pressure development in a non-Newtonian flow through a tapered tube, *Biorheology*, 10(2)(1973), 207-212.
- [10] Pappu V. and Bagchi P., Hydrodynamic interaction between erythrocytes and leukocytes affects rheology of blood in microvessels, *Biorheology*, 44(3)(2007), 191-215.

- [11] Pries A. R. and Secomb T. W., Resistance to blood flow in vivo, from poiseuille to the in vivo viscosity law, *Biorheology*, 34(4)(1997), 369-373.
- [12] Sakamoto K., Sunaga R., Nakamara K. and Sato Y., Study of the relation between fluid distribution change in tissue and impedance change in during hemodialysis by frequency characteristics of the flowing blood, *Annals N. Y. Acad. Sci.*, 873(1) (1999), 77-88, doi: 10.1111/j.1749-6632.1999.tb09452.x.
- [13] Singh N. L. and Kumar J., Mathematical study of steady blood flow in narrow vessel with plasma layer near the wall, *Indian Journal Theoretical Physics*, 50(2002), 155-160.
- [14] Womersley J. R., Method for the calculation of velocity rate of flow and viscous drag in the arteries when the pressure gradient is known, *J. Physiol*, 127(3)(1955), 553-563, doi: 10.1113/jphysiol.1955.sp005276.